II CONGRESSO NACIONAL DE ENGENHARIA MECÂNICA
II NATIONAL CONGRESS OF MECHANICAL ENGINEERING
12 a 16 de Agosto de 2002 - João Pessoa – PB

FREE CONVECTION HEAT TRANSFER IN SQUARE AND RECTANGULAR CAVITIES HEATED FROM BELOW OR ON THE LEFT

Edimilson Junqueira Braga
Marcelo J.S. De-Lemos*
Departamento de Energia, IEME
Instituto Tecnológico de Aeronáutica – ITA
12228-900 - São José dos Campos, SP – Brazil
* E-mail: delemos@mec.ita.br

Abstract. *Steady laminar natural convection in a two-dimensional square and rectangular cavities isothermally heated from below or the left and cooled from the opposing side is analyzed numerically using the finite volume method and compared with the De Vahl Davis' Bench Mark results. Governing equations are written in terms of primitive variables and are recast into a general form. Based on numerical predictions, the effects of Rayleigh number and aspect ratio on flow pattern and energy transport are investigated for Rayleigh numbers ranging from 10^3 to 10^6, and for three different aspect ratios, namely 0.25, 1.0 and 4.0. In general, the effect of Rayleigh number on heat transfer is found to be more significant when the enclosure is shallow. Also, the influence of aspect ratio is stronger when the enclosure is tall and the Rayleigh number is high.*

Keywords: *Cavity, Free Convection, buoyancy flow*

1. INTRODUCTION

The analysis of buoyancy-driven flows in an enclosed cavity provides useful comparisons for evaluating the robustness and performance of numerical methods dealing with viscous flow calculations. The importance of the enclosure natural-convection phenomena can best be appreciated by noting several of their application areas. The optimal design of furnaces and solar collectors - contributing to energy losses minimization - nuclear reactor safety and insulation, ventilation rooms and crystal growth in liquids are some examples of applications of heat removal or addition by free convection mechanism.

Natural convection occurs in enclosures as a result of gradients in density which, in turn, are due to variations in temperature or concentration. Natural convection in a infinite horizontal layer of fluid, heated from below, has received extensive attention since the beginning of the 20^{th} century when Bérnard (1901) observed hexagonal roll cells upon the onset of convection in molten spermaceti with a free upper surface. The work of Rayleigh (1926) was the first to compute a critical value, Ra_c, for the onset of convection. The accepted theoretical value of this dimensionless group is 1708 for infinite rigid upper and lower surfaces. The study of natural convection in enclosures still attracts the attention of researchers and a significant number of experimental and theoretical works have been carried out mainly from the 80's.

During the conference on Numerical Methods in Thermal Problems, which took place in Swansea, UK, Jones (1979) proposed that buoyancy-driven flow in a square cavity would be a suitable vehicle for testing and validating computer codes. Following discussions at Swansea, contributions for the solution of such problem were invited. A total of 37 contributions from 30 contributors or groups of contributors in nine countries were received. The summarization and

discussion of the main contributions yielded the benchmark of De Vahl Davis (1983) which is one of the most important reference works in this area.

2. THE PROBLEM CONSIDERED

The problem considered is showed schematically in Fig. (1) and refers to the two-dimensional flow of a Boussinesq fluid of Prandtl number 0.71 in a rectangular cavity of height H and width L. The cavity is assumed to be of infinite depth along the z-axis and is isothermally heated from below or the left and cooled from the opposing side. The other two walls in each case are insulated. The no-slip condition is applied on the velocity at all four walls and the resulting flow is treated as steady and assumed as laminar if the Rayleigh number, $\mathrm{Ra} = \frac{g\beta L^3 \Delta T}{\nu\alpha}$, is less than 10^6.

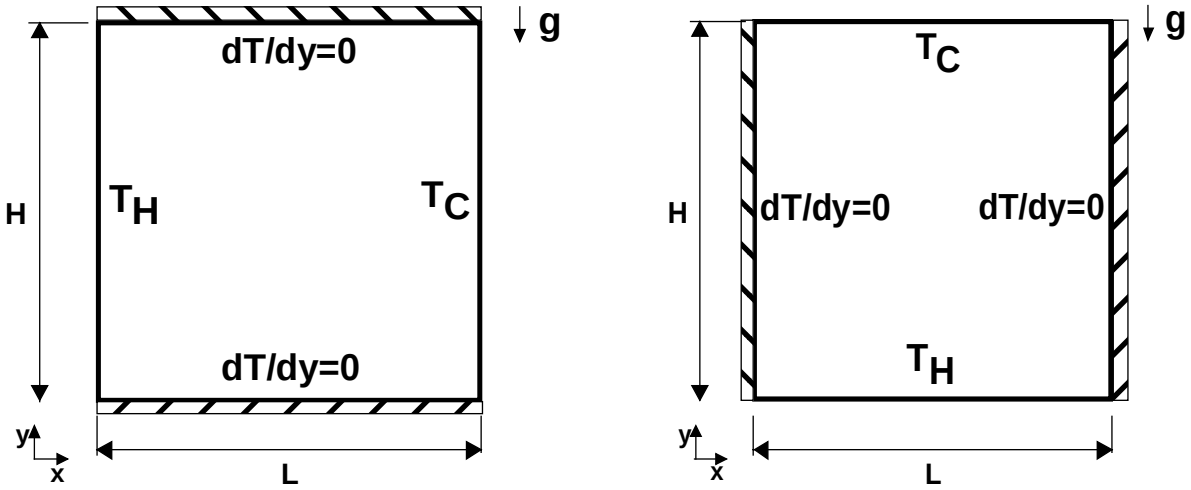

Figure 1. The cavities under consideration

3. MATHEMATICAL FORMULATION

3.1 The Differential equations

For steady flow, the equations for continuity, momentum and temperature take the form:

$$\frac{\partial u}{\partial x} + \frac{\partial v}{\partial y} = 0 \tag{1}$$

$$u\frac{\partial u}{\partial x} + v\frac{\partial u}{\partial y} = -\frac{1}{\rho}\frac{\partial P}{\partial x} + \nu\nabla^2 u \tag{2}$$

$$u\frac{\partial v}{\partial x} + v\frac{\partial v}{\partial y} = -\frac{1}{\rho}\frac{\partial P}{\partial y} + \nu\nabla^2 v + g\beta(T - T_o) \tag{3}$$

$$u\frac{\partial T}{\partial x} + v\frac{\partial T}{\partial y} = \alpha\nabla^2 T \tag{4}$$

where u and v are the velocity components in x and y directions, respectively, ρ is the density of the fluid, P is the total pressure and ν is the kinematic viscosity of the fluid. Gravity acceleration is defined by g and β is the thermal expansion coefficient. T and T_o are the local temperature and the

reference temperature, respectively, and α is the thermal diffusivity. Finally, L is the length of the gap and is taken as a characteristic length.

3.2 The Numerical Method and Solution Procedure

The numerical method employed for discretizing the governing equations is the control-volume approach with a collocated grid arrangement A hybrid scheme, mixing the Upwind Differencing Scheme (UDS) and the Central Differencing Scheme (CDS) is used for interpolating the convection fluxes. With the help of Fig. (2) the following operators can be identified:

$$\Delta x_{\eta}^{e} = (x_{ne} - x_{se}), \quad \Delta x_{\xi}^{e} = (x_{E} - x_{P}), \quad \Delta y_{\eta}^{e} = (y_{ne} - y_{se}), \quad \Delta y_{\xi}^{e} = (y_{E} - y_{P}), \tag{5}$$

$$\Delta x_{\xi}^{n} = (x_{ne} - x_{nw}), \quad \Delta x_{\eta}^{n} = (x_{N} - x_{P}), \quad \Delta y_{\xi}^{n} = (y_{ne} - y_{nw}), \quad \Delta y_{\eta}^{n} = (y_{N} - x_{P}). \tag{6}$$

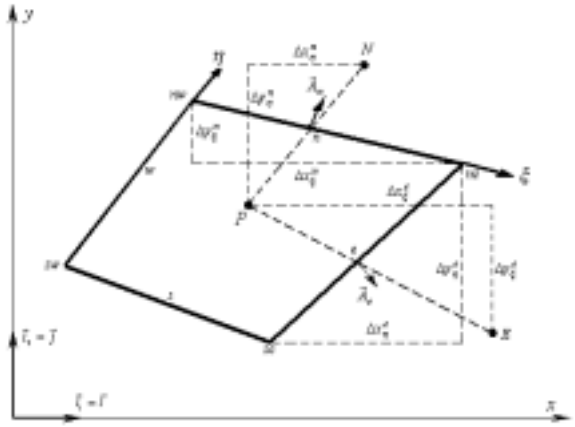

Figure 2. Control-volume and notation

It is important to emphasize that Eq. (5)-(6), derived from Fig. (2), are based on a generalization of the Cartesian grid employed for computing the flows in the cavities of Fig. (1). Herein, due to the simplicity of the geometry analyzed, the non-orthogonal boundary-fitted grid layout of Fig. (2) degenerates into a standard Cartesian mesh employed in the cavities shown in Fig (1).

Thus, the vector form of the area of the control-volume at *east* and *north* faces, respectively, are given by

$$\vec{A}_{e} = \Delta y_{\eta}^{e}\vec{i} - \Delta x_{\eta}^{e}\vec{j}, \qquad \vec{A}_{n} = -\Delta y_{\xi}^{n}\vec{i} + \Delta x_{\xi}^{n}\vec{j}. \tag{7}$$

The well-established SIMPLE, Patankar & Spalding (1972), is followed for the momentum equations which is solved by a line-by-line procedure namely SIP, Stone (1968).

3.3 The Nusselt Number

From the engineering viewpoint, the most important characteristic of the flow is the rate of heat transfer across the cavity. The Nusselt number on the hot wall at x=0 is given by,

$$Nu = \left(\frac{\partial T}{\partial x}\right)_{x=0} \frac{L}{T_H - T_C} \tag{8}$$

and the average Nusselt number is given by,

$$\overline{Nu} = \frac{1}{H}\int_{0}^{H} Nu\, dy \tag{9}$$

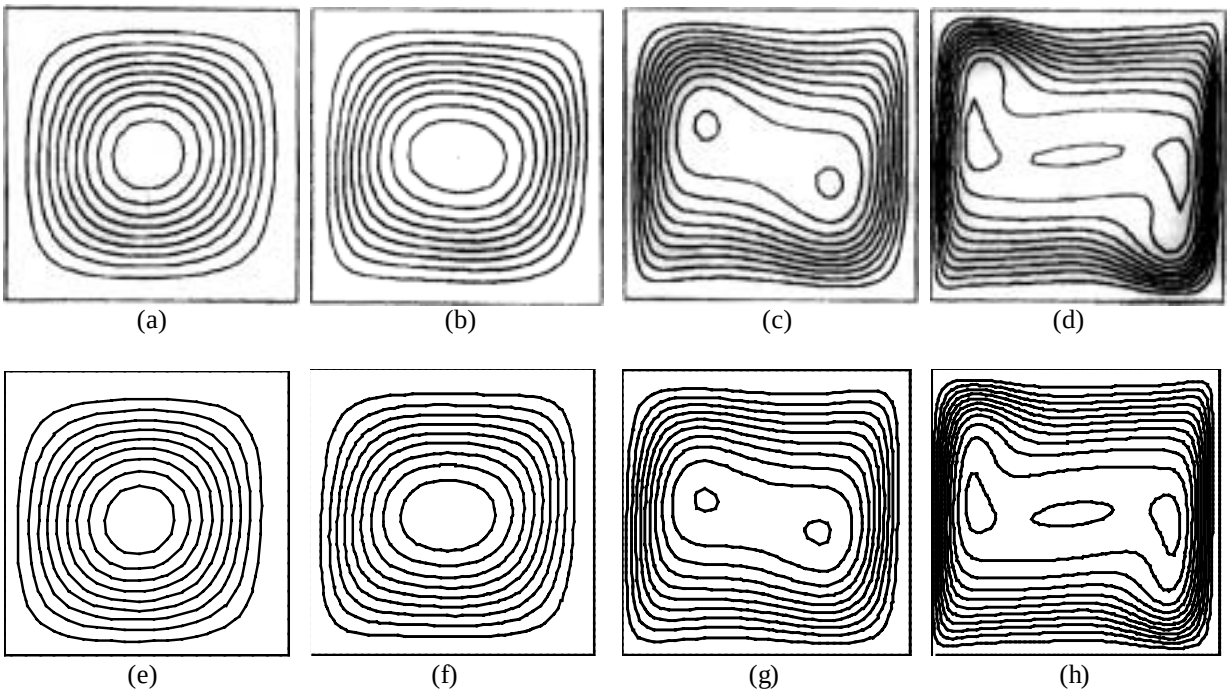

Figure 3. Streamlines for ($10^3 \leq Ra \leq 10^6$), De Vahl **Davis (1983)**, (a), (b), (c) and (d), Present Results, (e), (f), (g) and (h).

4. RESULTS AND DISCUSSION

4.1 Vertical Cavities

Figure (3) shows the streamlines of a square cavity heated on the left and cooled from the opposing side for Rayleigh numbers ranging from 10^3 to 10^6.

At $Ra=10^3$, the streamlines in Fig. (3a) indicates the existence of a single vortex with center in the middle of the cavity. Corresponding Isotherms, Fig. (4a), are almost parallel to the heated walls, indicating that most of the heat transfer is transferred by conduction. The vortex is generated due the horizontal temperature gradient across the section. This gradient, $\partial T/\partial y$, is negative everywhere, inducing a clockwise oriented vorticity.

When the Rayleigh number is increased to $Ra=10^4$, Fig. (3b), the central vortex is distorted into an elliptic shape and the effect of convection is more pronounced in the isotherms, Fig. (4b). Temperature gradients are stronger near the vertical walls, but decrease in the center region. For $Ra=10^5$, Fig. (3c), the behavior continues. The central vortex is elongated and two secondary vortices appear inside it.

Heat transfer by convection in the viscous boundary layer alters the temperature distribution to such an extent that temperature gradients in the center of the domain are close to zero. Fig. (4c) shown that, with this change in the sign of the source term, negative vorticity is induced within the domain. This also causes the development of secondary vortices in the core.

Accordingly the work of Markatos & Pericleous (1984), the secondary vortices in the square cavity do not result from an instability of the base flow but are a direct consequence of the convective distortion of the temperature field. As Ra increases, the development of thermal boundary layers intensifies $\partial T/\partial y$ in the vicinity of the walls, and the convection within each layer leads to negative $\partial T/\partial y$ at the center.

Finally, increasing Ra to 10^6, Fig. (3d), causes the secondary vortices to move closer towards the walls and are convected further downstream. A third vortex appears in center of the domain rotating clockwise instead, reducing the shear stress between the other two vortices. The work of Mallinson

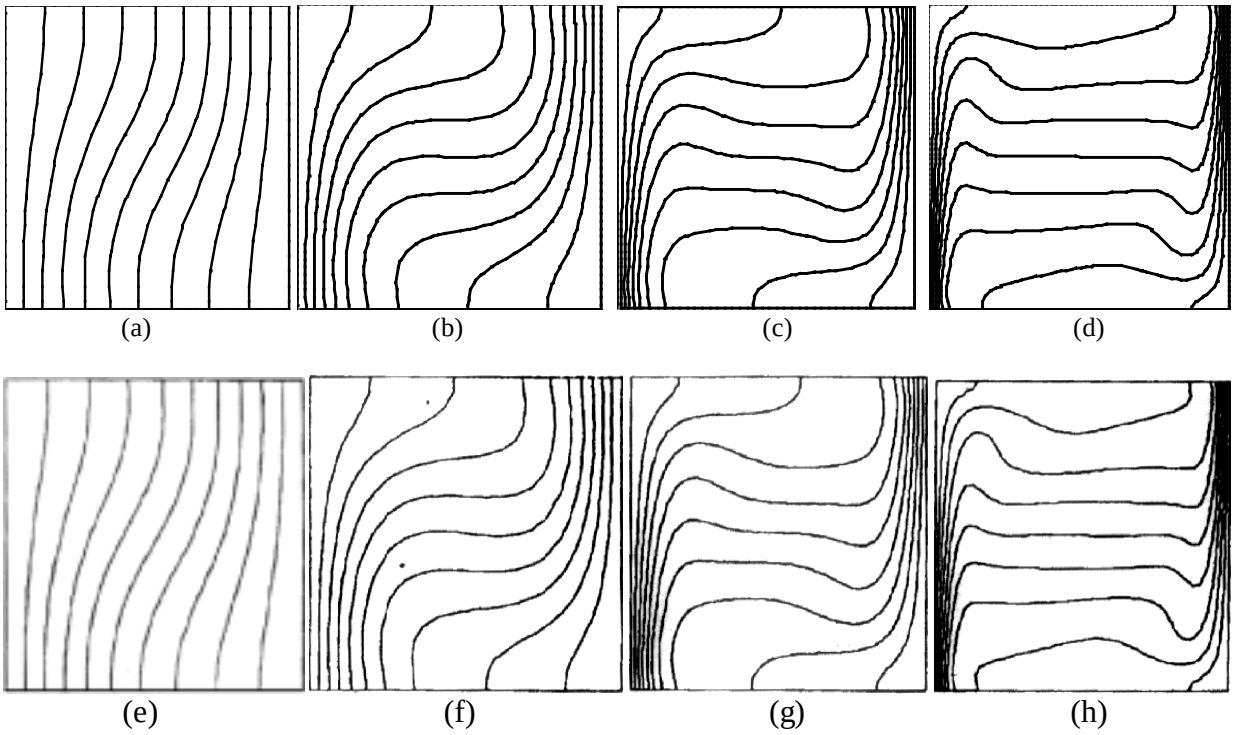

Figure 4. Isotherms for ($10^3 \leq Ra \leq 10^6$), Present Results, (a), (b), (c) and (d), De Vahl **Davis (1983)**, (e), (f), (g) and (h).

& Davis (1977) attribute this to the presence of a small positive temperature gradient in the center of the cavity, causing the viscous diffusion between the secondary vortices to dissipate any counterclockwise vortices that might eventually appear. Ultimately, Fig. (4d), heat transfer is now mostly by convection in the fast moving fluid near the walls.

Table (1) shows, for the four Rayleigh numbers here analyzed and for the various mesh sizes used, the following quantities:

$\overline{Nu}$ the average Nusselt number on the vertical boundary of the cavity at x=0;
Nu_{max} the maximum value of the local Nusselt number on the boundary at x=0;
Nu_{min} the minimum value of the local Nusselt number on the boundary at x=0.

Table 1. Nusselt numbers for Rayleigh numbers ranging from 10^3 to 10^6.

	Ra = 10^3		Ra = 10^4		Ra = 10^5		Ra = 10^6	
		Error(%)		Error(%)		Error(%)		Error(%)
$\overline{Nu}$	1.140	2.06	2.279	1.83	4.749	5.32	9.410	6.72
Nu_{max}	1.528	1.53	3.665	3.88	8.496	10.09	20.267	13.06
Nu_{min}	0.727	5.06	0.729	5.46	0.844	15.77	1.229	24.27
Mesh Size	20 x 20		40 x 40		40 x 40		60 x 60	

The values shown in Tab. (1) agree well with the benchmark with a maximum error of 6.72% for the average Nusselt number for $Ra=10^6$.

The heat transfer coefficient is seen to increase with Rayleigh number, as convection becomes dominant, but not as fast as the flow. The maximum Nusselt number occurs at the bottom of the cavity and the minimum at the top. Differences exist in the minimum Nusselt number, particularly at $Ra=10^6$. Although the agreement of the maximum and average coefficient is relatively good, the present predictions indicate a higher minimum Nusselt number than the benchmark solution. The

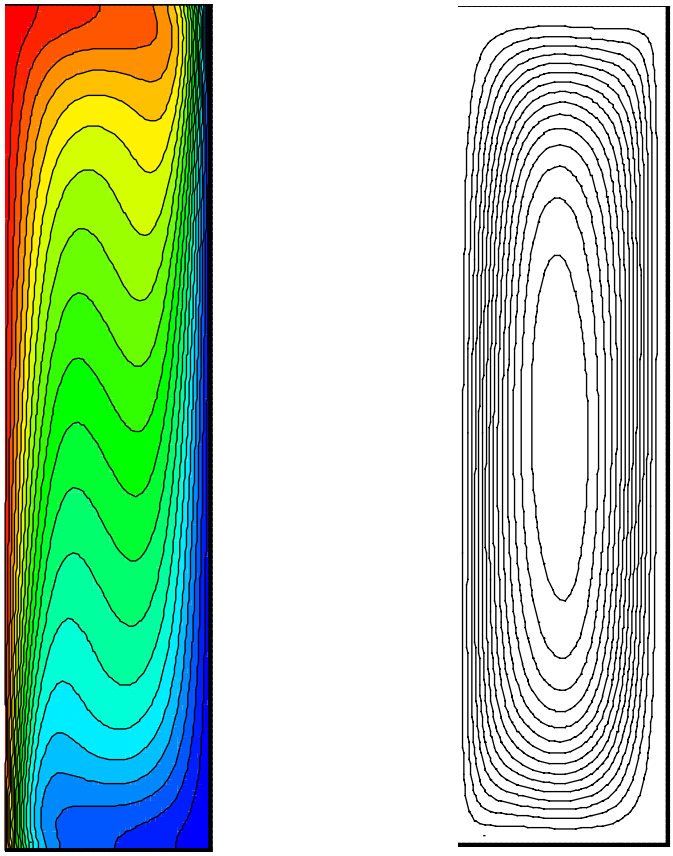

(a) (b)

Figure 5 – Effect of H/L=4 on temperature distribution and streamlines for cavity heated from left.

large errors in the calculation of the minimum Nusselt number appear to be due to the sensitivity of its calculation to grid size and to the discretization of the convection term.

The effect of the aspect ratio H/L=4 is shown in Fig. (5) for Rayleigh equal to $4.x10^4$ and H/L equal to 4. The three flow regimes known in the literature Churchill (1992), namely, the boundary-layer type, the transition, and conduction regimes as H/L increases, are not fully simulated here due to the relatively small Ra used and the narrow range for H/L. The solution for Fig. (5) seems to be a representative of boundary layer regime for this Rayleigh, having a somewhat stratified core and a uni-cell flow structure. As the H/L ratio increases (not shown here), flow stratification prevails over most of the domain and the conduction mechanism controls heat transfer.

Accordingly the work of de Lemos (2000), it is also interesting to note that as H/L increases the major flow currents changes from horizontal to vertical and the core of the flow becomes mostly stratified. Also, a reduction on average temperature gradient at the wall, due to stratification, decreases the Nusselt number, ultimately leading to the mentioned conduction-dominated regime

4.2 Horizontal Cavities

Figure (6a) below shows that for small values of Rayleigh number, only a slight departure from the purely conduction regime is detected, most likely due to the weak circulation computed and the flow becomes stratified. As Ra increases to $4.x10^4$, Fig. (6b), the circulatory motion brings the bottom hot temperature stream up to the top wall, substantially penetrating into the flow core. Finally, a further increase in Ra to $1.x10^5$, Fig (6f), destroys the double-swirl pattern and the flow becomes a of single vortex type. An increase in the value Ra around 10^6 seems to reach the instability regime and further increases in Ra would lead to the turbulent regime, which cannot be computed with the mathematical model herein.

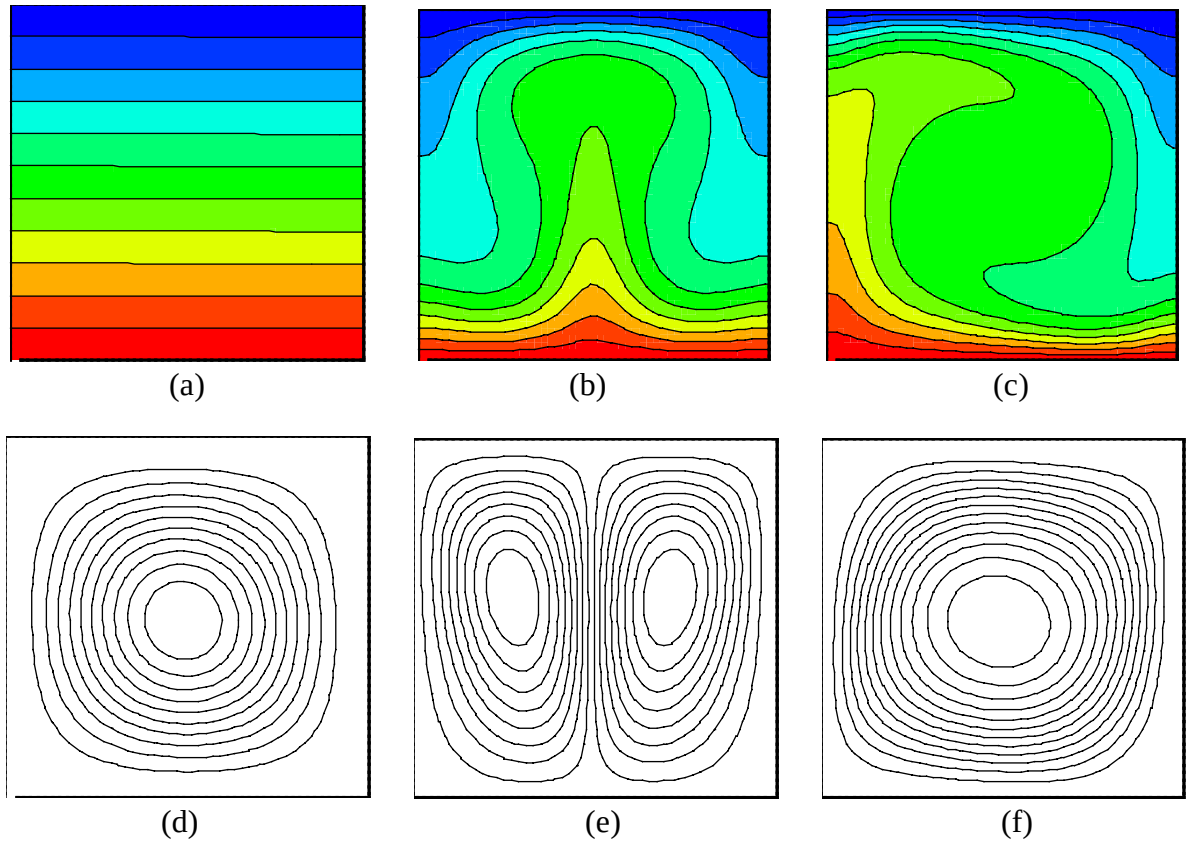

Figure 6 - Isotherms for (Ra=10^3, 4.x10^4, 10^5), (a), (b), (c) and streamlines respectively.

In Fig. (7) longer cavities are analyzed with H/L=0.25 and Ra=4.10^4 The figure shows temperature distribution and streamlines for cavity heated from the bottom, indicating a repetitive structure of the one presented in Fig. (6b). The longer shape of the rectangular cavity breaks the flow recirculatory motion into many vortexes in order to exchange heat from the surfaces at different temperatures. In general, the effect of Rayleigh number on heat transfer is found to be more significant when the enclosure is shallow and the influence of aspect ratio is stronger when the enclosure is tall and the Rayleigh number is high.

5. CONCLUSIONS

Natural convection in 2-D square and rectangular cavities heated from below or on the left has been analyzed numerically using a control volume technique. Calculation has been performed for laminar flow for a number of Ra up to 10^6**.** Accurate results have been obtained after grid independence studies were conducted. The solution captures very well all flow and heat transfer phenomena, especially near the walls.

The present results compare favorably with benchmark solutions for the laminar case for all Rayleigh numbers analyzed, as well as the Nusselt number along the hot wall. In general, the effect of Rayleigh number on heat transfer is found to be more significant when the enclosure is shallow and the influence of aspect ratio is stronger when the enclosure is tall and the Rayleigh number is high.

Although only time-average steady-state results have been presented, the numerical procedure herein can also be used for simulating transient flows. Also, radiation and variable property effects and turbulence, that have been neglected in the present work, must be included to investigate their importance as the Rayleigh number increases.

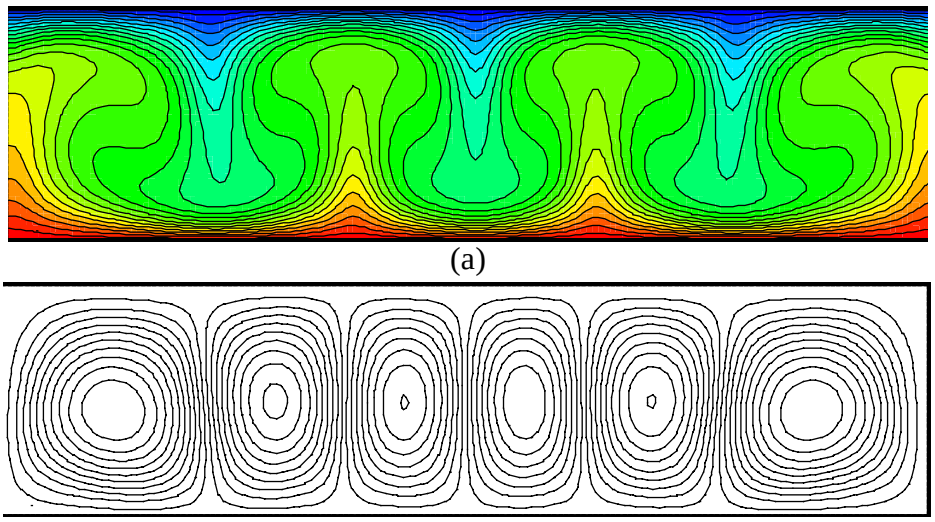

(a)

(b)

Figure 7 - Effect of H/L=0.25 on temperature distribution and streamlines for cavity heated from the bottom.

6. ACKNOWLEDGEMENTS

The authors are thankful to CNPq, Brazil, for their financial support during the course of this research.

7. REFERENCES

Bérnard, H., 1901, Les Tourbillons cellulaires dans une nappe liquide transportant de la chaleur par convection em régime permanent, Ann. Chim. Phys., vol 23, pp. 62-144.

Churchill, S., 1992, Free convection in layers and enclosures, in Hewitt G. F. (ed.), Handbook of Heat Exchanger Design, Chap 2.5.8.

De Vahl Davis, G., Jones, I. P., 1983, Natural convection in a square cavity – A comparison exercise, Int. J. Num. Methods in Fluids, Vol 3, pp. 227-248.

De Vahl Davis, G., 1983, Natural convection in a square cavity: A benchmark numerical solution, Int. J. Num. Methods in Fluids, Vol 3, pp. 249-264.

De Lemos, M. J. S., 2000, Flow and heat transfer in rectangular enclosures using a new block-implicit numerical method, Numerical Heat Transfer, Part B, pp. 1-20.

Jones, I. P., 1979, A comparison problem for numerical methods in fluid dynamics: the double-glazing problem, Numerical Methods in Thermal Problems, R. W. Lewis and K. Morgan (cds.), Pineridge Press, Swansea, U.K., pp. 338-348.

Mallinson, G. D., Davis, G. V., 1977, Three-dimensional natural convection in a box: a numerical study, Int. J. Fluid Mech., Vol 83, pp. 1-31.

Markatos, N. C., Pericleous, K. A., 1984, Laminar and turbulent natural convection in an enclosed cavity, Int. J. Heat Mass Transfer, Vol 27, pp. 755-772

Patankar, S. V., Spalding, D. B., 1972, A calculation procedure for heat, mass and momentum transfer in three dimensional parabolic floews, Int. J. Heat Mass Transfer, Vol 15, pp. 1787.

Rayleigh, Lord (J. W. Strutt), 1926, On convection currents in a horizontal layer of fluid when the higher temperature is on the underside, Phil. Mag., ser. 6, Vol 32, pp.833-844.

Stone, H. L., 1968, Iterative Solution of Implicit Approximations of Multi-Dimensional Partial Differential Equations, SIAM J. Num. Anal., Vol 5, pp. 530-558.